Proposal of an ultra-compact mode multiplexer using air-hole type photonic crystal waveguides

Han Wang
Graduate School of Information Science and Technology
Hokkaido University
Sapporo, Japan
ORCID: 0000-0002-3135-5328

Takeshi Fujisawa
Graduate School of Information Science and Technology
Hokkaido University
Sapporo, Japan
ORCID: 0000-0002-1901-5531

Takanori Sato
Graduate School of Information Science and Technology
Hokkaido University
Sapporo, Japan
ORCID: 0000-0001-8460-6162

Kunimasa Saitoh
Graduate School of Information Science and Technology
Hokkaido University
Sapporo, Japan
ORCID: 0000-0001-9622-1825

Abstract: *We propose an ultra-compact TE_0-TE_1 mode-division multiplexer based on air-hole photonic crystal waveguides. The longitudinal sizes are only 2.05 μm, which is 1/5 compared with that based on conventional Si-wire waveguides.*

Keywords: *Photonic crystal, Mode multiplexer, Space division multiplexing, Mode division multiplexing*

I. Introduction

With the rapid increase in Internet traffic, the demand for communication capacity expansion of optical fiber is increasing. Since the 1980s, optical fiber communication technology has experienced several technological innovations, and the development of multiplexing technologies such as wavelength division multiplexing (WDM) has increased the communication capacity of single-mode fiber. However, the communication capacity of conventional single-mode optical fiber is approaching its limit [1]. The mode division multiplexing (MDM) transmission, which is one of the space division multiplexing (SDM) technologies, has received attention [2]. MDM can further expand the transmission capacity by using multiple spatial modes propagating in one optical waveguide as transmission channels. Combining WDM and MDM technologies is effective in expanding transmission capacity from long-distance fiber communication to very-short-reach chip-based communication. WDM/MDM hybrid multiplexing technology that can realize wavelength and mode division multiplexing at the same time was proposed [3-5].

For chip communications, the size of the device is an important indicator to achieve high integration density. Nanophotonic technologies based on Si wire waveguides and photonic crystals can confine light to smaller devices due to the high refractive index difference of materials. These technologies have become candidates for reducing the size of optical devices [3-7]. Photonic crystals (PC) are widely studied because of their unique performance and high integration density [6,7]. In some studies of WDM/MDM hybrid multiplexers (MUXs), WDM and MDM parts adopt different structures, WDM parts use hole-type PC, and MDM use Si wire waveguides [3]. In this case, the loss will occur in the connection part of the PC and Si waveguide. Therefore, all PC mode MUX is desired to integrate all components for chip communications with PC waveguides (PCWs). However, at present, mode MUXs based on 2-D pillar-type PCWs have been investigated [4,5,8], which are not realistic from a manufacturing point of view.

In this study, we propose ultracompact mode MUX based on the air-hole type PCW which have more practical applications. By using asymmetric directional coupler (ADC), it is possible to compose TE_0-TE_1 mode MUX by changing the waveguides widths. The longitudinal sizes are only 2.05 μm, which is significantly smaller than those based on Si-wire waveguides.

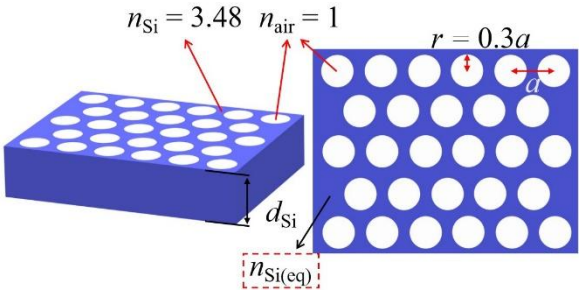

Fig. 1 The schematic diagrams of the 3D PC structure (left) and its plane view (right).

II. Air-hole Photonic Crystal

The schematic diagrams of the 3D PC structure and its plane view considered in this study are shown in Fig. 1. It consists of Si plate with the thickness of d_{Si}. Air-holes with the radius of r are arranged in triangular lattice with the lattice constant of a. The refractive index of the 3D Si slab is set to n_{Si} = 3.48. Here, we examine an equivalent 2D structure with the equivalent refractive index $n_{Si(eq)}$, because the purpose of this work is to show the theoretical possibility of mode MUX based on air-hole PCWs, which have not been considered yet.

The equivalent 2D structure to the 3D structure is determined as follows. In this study, all the calculations were done with FDTD. Figure 2 (a) shows normalized frequencies (a/λ) of the upper edge, center, and lower edge of the photonic bandgap (PBG) for 2D PC as a function of $n_{Si(eq)}$. Figure 2 (b) shows the same one for 3D PC as a function of d_{Si}. Figure 2 (a) and (b) are calculated under the parameters of a = 0.41 μm and r = 0.3a. For both Figures, the PBG widths are also plotted for the right axis. The PBG width and the position are changed with the parameters. Figure 3 (a) shows the 2D and 3D PBG width as a function of $n_{Si(eq)}$ (lower horizontal axis) and d_{Si} (upper horizontal axis). The 3D PBG width is not so changed with d_{Si}, while the 2D PBG width has its maximum around $n_{Si(eq)}$ = 3.037, where the difference between 2D and 3D PBGs is small. To ensure that the higher-order mode and the fundamental mode can appear simultaneously in the PBG, we selected the widest 2D PBG when the $n_{Si(eq)}$ = 3.037 as the parameter for subsequent calculation. Figure 3 (b) shows the 2D and 3D normalized frequency at the center of the PBGs as a function of $n_{Si(eq)}$ and d_{Si}. The center frequency of the 3D PC at d_{Si} = 460 nm is equal to the center frequency of the 2D PC at $n_{Si(eq)}$ = 3.037,

where the PBG widths are also similar between 2D and 3D PCs. Therefore, a 3D PC with d_{Si} = 460 nm can be well approximated by a 2D PC with $n_{Si(eq)}$ = 3.037. PBG parameters for these 2D and 3D PCs are summarized in Table 1, and hereafter, we use them for the 2D equivalent PC. It should be noted that 3D PBG width is slightly larger for smaller values of d_{Si}, as shown in Fig. 3 (a) (although the difference is very small). Therefore, there is a possibility that thinner Si slab will lead to better performance in 3D design. However, as stated above, the purpose of this paper is to show mode multiplexing possibility in air-hole PCWs, and therefore, we used above parameters in this work. Full optimization of 3D structure will be reported elsewhere.

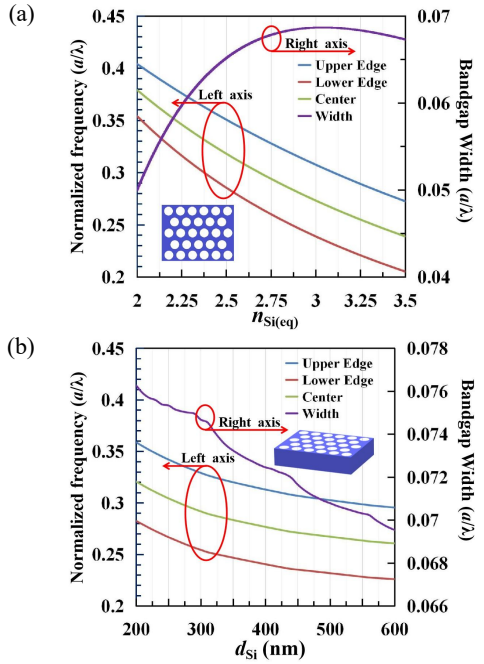

Fig. 2 (a) 2D PBG structure as a function of $n_{Si(eq)}$ and (b) 3D PBG structure as a function of d_{Si}, where a = 0.41 μm and r = 0.3a.

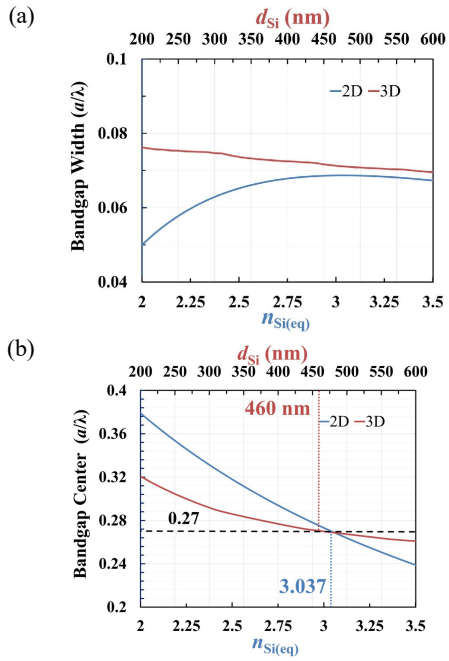

Fig. 3 (a) PBG width and (b) PBG center frequency of 2D and 3D PCs, where a = 0.41 μm and r = 0.3a.

Table 1 Bandgap parameters (a/λ)

r = 0.3a	2D structure	3D structure
	$n_{Si(eq)}$ = 3.037	d_{Si} = 460 nm
Upper edge	0.30463	0.30605
Lower edge	0.23596	0.23465
Center	0.27029	0.27035
Width	0.06868	0.07141

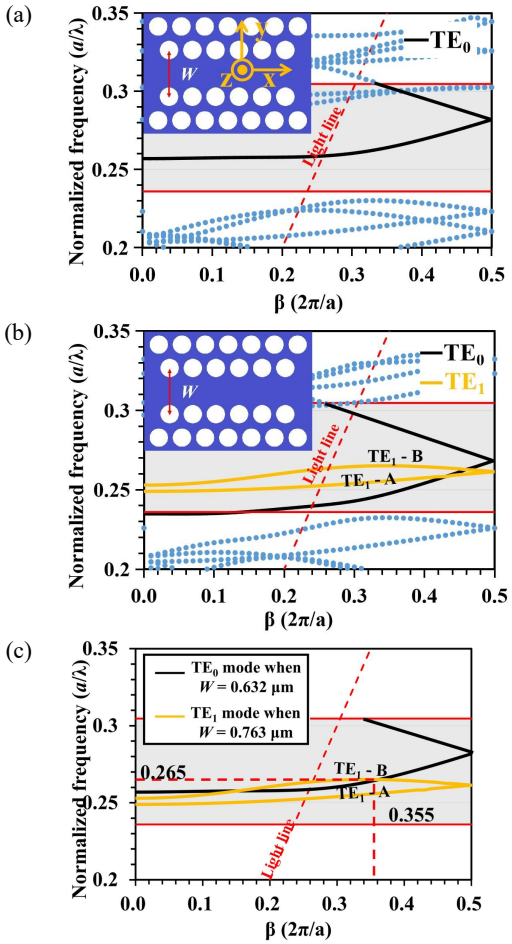

Fig. 4 Dispersion curves of the PCW with W = (a) 0.632 μm, (b) 0.763 μm, and (c) the dispersion curves of PCWs in Fig. 4 (a) and (b) superimposed on the same Figure, where a = 0.41 μm.

III. Air-hole Photonic Crystal Waveguides

Once the PC structure is determined, the next task is to investigate the guided modes. A line defect with the width of W is introduced into a complete PC by removing an array of air holes, forming a PCW. Hereafter, the lattice constant is set to a = 0.41 μm. For this lattice constant, normalized frequency of 0.265 corresponds to a wavelength of 1550 nm. Figure 4 (a) shows the dispersion curve of the PCW with W = 0.632 μm. The hatched area is the PBG. The waveguide is single-mode for the normalized frequency from 0.259 to 0.282 under the light line. Here, we define the xyz coordinate as shown in the inset of Fig. 4(a), and TE mode is defined as the modes, whose principal electromagnetic components are H_z, E_x, and E_y. Figure 4 (b) shows the dispersion curve of the PCW with W = 0.763 μm. By increasing the width, a higher-order mode (TE_1) appears in the PBG. There are two curves for the mode and labeled as TE_1-A and -B modes. They are also under the light line and can be used for the guided mode. Figure 4 (c) shows the dispersion curves of PCWs with W = 0.632 and 0.763 μm superimposed on the same Figure (Here,

we only focus on the TE_0 mode when W = 0.632 μm and the TE_1 modes when W = 0.763 μm). The TE_0 mode of the single-mode waveguide and the TE_1-B mode of the multimode waveguide have an intersection point at the normalized frequency of 0.265, and the propagation constant β of the two modes are both 0.355. Therefore, the TE_1 mode can be excited by using the phase matching conditions [9].

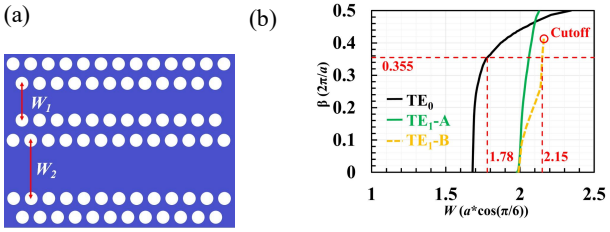

Fig. 5 (a) Mode multiplexer structure. (b) Relationship between propagation constant β and the waveguide width W at a/λ = 0.265.

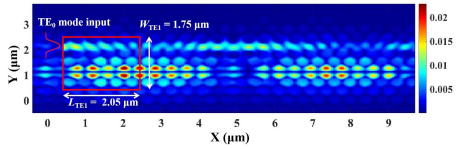

Fig. 6 Magnetic field distribution $|H_z|$ of TE_0-TE_1 mode MUX at a/λ = 0.265.

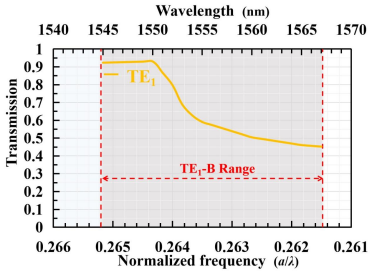

Fig. 7 Transmission spectrum of TE_1 mode MUX.

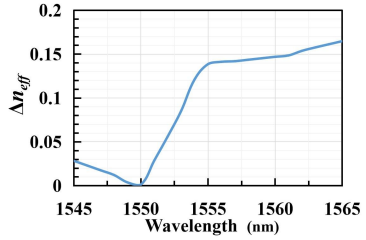

Fig. 8 Δ*neff* spectrum.

IV. Ultracompact Photonic Crystal Mode Multiplexer

Here, we consider a mode MUX based on an ADC. It consists of a single-mode waveguide with the width of W_1 and a multi-mode waveguide with the width of W_2 arranged in parallel as shown in Fig. 5(a). Two rows of air-holes are placed between two waveguides and the separation between two waveguides is 0.355 μm. Figure 5 (b) shows the propagation constant β of TE_0 and TE_1 modes as a function of the waveguide width W at a/λ = 0.265 (λ = 1550 nm for a = 0.41 μm). For the TE_0 mode with W_1 = 1.78*(a*cos(π/6)) = 0.632 μm, the phase matching conditions are satisfied for TE_1 mode with W_2 = 2.15*(a*cos(π/6)) = 0.763 μm. Figure 6 shows the field distribution of TE_0-TE_1 mode MUX, where W_1 and W_2 are 0.632 and 0.763 μm, at the wavelength 1550 nm. As we can see, the TE_0 mode launched from narrow waveguide is coupled to the TE_1 mode of wide waveguide. The coupling length is only 2.05 μm for the lattice constant a = 0.41 μm. The typical coupling length for the ADC based on Si-wire waveguides with the waveguide separation of 200 nm around 1550 nm is about 10 μm [10]. Here, the coupling length of proposed PCW ADC is 1/5 even though the waveguide separation is increased to 0.355 μm. Figure 7 shows the calculated transmission spectrum of the TE_1 mode MUX for the lattice constant a = 0.41 μm. Since the TE_1-B mode only exists in the normalized frequency range of a/λ = 0.2615 ~ 0.2652, we only show the results in the range, where the TE_1-B mode exists. The transmissions of the TE_1 mode at the wavelength of 1550 nm are greater than 90%. However, the transmissions at other wavelengths are degraded, especially for longer wavelength region. This partly comes from that the phase matching condition is not satisfied for the other wavelength region. Figure 8 shows the effective index difference, Δn_{eff} spectrum between TE_0 and TE_1-B modes. Δn_{eff} is zero at 1550 nm and is not zero for other wavelengths, and the value is large for longer wavelength side. Therefore, the phase mismatch seems to be the dominant factor for longer wavelength side degradation.

V. Conclusions

We proposed an ultra-compact air-hole PC mode MUX using waveguide phase matching principle. It was shown that the two mode (TE_0 and TE_1 modes) multiplexing is possible, the size of the MUX can be reduced to 1/5 compared with those of Si-wire based mode MUX, and more than 90% transmission is possible at the wavelength of 1550nm.

Acknowledgment

This work was supported by JST SPRING, Grant Number JPMJSP2119.

References

[1] T. Morioka, "New generation optical infrastructure technologies: 'EXAT initiative' towards 2020 and beyond," *Optoelectron. Commun. Conf. OECC*, p. 1, 2009.

[2] T. Morioka, Y. Awaji, R. Ryf, P. Winzer, D. Richardson, and F. Poletti, "Enhancing optical communications with brand new fibers," *IEEE Commun. Mag.*, vol. 50, no. 2, p. 31, 2012.

[3] Y. Zhuang, H. Chen, K. Ji, and Y. Hu, "On-chip hybrid demultiplexer for mode and coarse wavelength division multiplexing," *Appl. Phys. B Lasers Opt.*, vol. 125, no. 12, 2019.

[4] K. Ji, H. Chen, Y. Zhuang, and W. Zhou, "A hybrid multiplexer/de-multiplexer for wavelength-mode-division based on photonic crystals," *J. Mod. Opt.*, vol. 65, no. 14, p. 1623, 2018.

[5] O. M. Nawwar, H. M. H. Shalaby, and R. K. Pokharel, "Photonic crystal-based compact hybrid WDM/MDM (De)multiplexer for SOI platforms," *Opt. Lett.*, vol. 43, no. 17, p. 4176, 2018.

[6] Y. Zhang, Y. Zhang, and B. Li, "Optical switches and logic gates based on self-collimated beams in two-dimensional photonic crystals," *Opt. Express*, vol. 15, no. 15, p. 9287, 2007.

[7] E. Tresa, P. Mankar, and J. Digge, "Silicon based 2D Photonic Crystal Power Splitter for Optical Network," *Proceeding - 1st Int. Conf. Innov. Trends Adv. Eng. Technol. ICITAET*, p. 144, 2019.

[8] W. Zhou, Y. Zhuang, K. Ji, and H. Chen, "Multi/demulti-plexer based on transverse mode conversion in photonic crystal waveguides," *Opt. Express*, vol. 23, no. 19, p. 24770, 2015.

[9] K. Saitoh, N. Hanzawa, T. Sakamoto, T. Fujisawa, Y. Yamashita, T. Matsui, K. Tsujikawa, and K. Nakajima, "PLC-based mode multi/demultiplexers for mode division multiplexing," *Opt. Fiber Technol.*, vol. 35, p. 80, 2017.

[10] Y. Sawada, T. Fujisawa, and K. Saitoh, "Broadband and compact silicon mode converter designed using a wavefront matching method," *Opt. Express*, vol. 28, no. 25, p. 38196, 2020.